ANNALS OF
BOTANY
Founded 1887

Combining FISH and model-based predictions to understand chromosome evolution in *Typhonium* (Araceae)

Aretuza Sousa*, Natalie Cusimano and Susanne S. Renner

Department of Biology, University of Munich (LMU), D-80638 Munich, Germany
* For correspondence. E-mail: aretuzasousa@gmail.com

• *Background and Aims* Since the advent of molecular phylogenetics, numerous attempts have been made to infer the evolutionary trajectories of chromosome numbers on DNA phylogenies. Ideally, such inferences should be evaluated against cytogenetic data. Towards this goal, we carried out phylogenetic modelling of chromosome number change and fluorescence *in situ* hybridization (FISH) in a medium sized genus of Araceae to elucidate if data from chromosomal markers would support maximum likelihood-inferred changes in chromosome numbers among close relatives. *Typhonium*, the focal genus, includes species with $2n = 65$ and $2n = 8$, the lowest known count in the family.
• *Methods* A phylogeny from nuclear and plastid sequences (96 taxa, 4252 nucleotides) and counts for all included species (15 of them first reported here) were used to model chromosome number evolution, assuming discrete events, such as polyploidization and descending or ascending dysploidy, occurring at different rates. FISH with three probes (5S rDNA, 45S rDNA and *Arabidopsis*-like telomeres) was performed on ten species with $2n = 8$ to $2n = 24$.
• *Key Results* The best-fitting models assume numerous past chromosome number reductions. Of the species analysed with FISH, the two with the lowest chromosome numbers contained interstitial telomeric signals (*Its*), which together with the phylogeny and modelling indicates decreasing dysploidy as an explanation for the low numbers. A model-inferred polyploidization in another species is matched by an increase in rDNA sites.
• *Conclusions* The combination of a densely sampled phylogeny, ancestral state modelling and FISH revealed that the species with $n = 4$ is highly derived, with the FISH data pointing to a Robertsonian fusion-like chromosome rearrangement in the ancestor of this species.

Key words: Ancestral trait reconstruction, 5S rDNA, 45S rDNA, telomeres, FISH, Bayesian inference, maximum likelihood inference, aneuploid chromosome numbers, chromosome evolution, *Typhonium*, Araceae.

INTRODUCTION

Araceae are a large family of monocotyledons (3300 species, 117 genera; Boyce and Croat, 2013) that are phylogenetically well understood (Cusimano *et al.*, 2011; Nauheimer *et al.*, 2012). Many of the species are in cultivation, and chromosome counts are available for 862 species (26 % of the family), ranging from $2n = 10$ to $2n = 168$ (Cusimano *et al.*, 2012*a*: Supplementary Data Table S1 provides species names and original references). The family's range of chromosome numbers, phylogenetic framework and often easy cultivation (i.e. access to root tips) make Araceae suitable for bringing together modern methods of cytogenetics and ancestral trait reconstruction to advance our understanding of genome evolution and organization. As a first step, we recently inferred chromosome evolution using a genus-level phylogeny and maximum likelihood models of chromosome number change (Cusimano *et al.*, 2012*a*; model details are given in the Materials and Methods). The results suggested an ancestral haploid number of 16 or 18, rather than the base numbers of $x = 7$ (Larsen, 1969; Marchant, 1973) or $x = 14$ (Peterssen, 1993) previously hypothesized without consideration of phylogenetic relationships and probably overweighting derived chromosome numbers because the early-branching groups, such as Lemnoideae, which have relatively high chromosome numbers, were not yet included in Araceae. Other results

were a limited role for polyploidization and numerous reductions of chromosome numbers.

Typhonium, a Southeast Asian clade of 50–60 species, has already been the focus of studies in our lab treating its circumscription, natural geographic range and diversification rate (Cusimano *et al.*, 2010, 2012*b*). Prior to the present study, chromosome counts were available for only 10 of its species and ranged from $2n = 10$ (in *Typhonium baoshanense* and *T. jinpingense*; Zhonglang *et al.*, 2002; Zhin-Lin *et al.*, 2007) to $2n = 65$ [*Typhonium roxburghii*, Cusimano *et al.*, 2012*a*; Index to Plant Chromosome Numbers (IPCN) www.tropicos. org/Project/IPCN]. For the present study, we added new chromosome counts for another 15 species of the genus. *Typhonium* is embedded among genera with chromosome numbers based on $n = 13$ or 14 (*Arisaema*, *Pinellia*, *Sauromatum*, *Biarum*, *Helicodiceros*, *Dracunculus* and *Arum*); only *Theriophonum* has $n = 8$. In our family-wide study, which included just one species per genus, we inferred a reduction from an ancestral number $a = 14$–13 in this group (Cusimano *et al.*, 2012*a*). We here enlarge the phylogeny for *Typhonium* and its relatives and use the new and published chromosome counts to understand the chromosomal changes at a finer scale.

To achieve this, we selected ten species for fluorescence *in situ* hybridization (FISH) experiments, chosen to represent the range from $2n = 24$ to $2n = 8$, the lowest number in the family (newly

reported in this study). By applying three probes, 5S rDNA, 45S rDNA and an *Arabidopsis*-type telomeric probe – and with the more densely sampled phylogeny with more counted species – we hoped to test the previously inferred direction from higher to lower numbers via chromosome 'loss' and to be able to infer mechanisms behind numerical changes. Mechanisms detectable with FISH are structural changes associated with primary chromosome rearrangements (insertions, deletions, duplications, reciprocal translocations and sequence amplification) or secondary chromosome rearrangements (replication slipping) (Schubert, 2007). Recent examples of such inferences based on FISH come from *Hypochaeris* and *Nothoscordum arenarium* (Weiss-Schneeweiss *et al.*, 2008; Souza *et al.*, 2009). FISH can also help detect recent polyploidization, i.e. duplication of an organism's entire set of chromosomes, or dysploidy, i.e. an increase or decrease in chromosome number related to chromosome rearrangements, especially when used in a phylogenetic framework. For instance, the number of 5S rDNA and 45S rDNA sites sometimes doubles with polyploidization (Ansari *et al.*, 2008; Weiss-Schneeweiss *et al.*, 2008; Souza *et al.*, 2010). Similarly, decreasing dysploidy inferred from a phylogeny would be supported by the discovery of interstitial telomeric signals. Such signals are sometimes found following fusion–fission cycles, and with probes homologous to plant telomeric repeats they can be visualized (Schubert, 1992; Fuchs *et al.*, 1995). Since several mechanisms can lead to interstitial telomere signals, a careful consideration of the specific karyotype(s) being analysed is always required, but in principle the distribution of telomeric signals can suggest chromosome loss by fusion.

MATERIALS AND METHODS

Sampling of taxa and molecular markers

We sampled the 96 species and subspecies of Areae tribe plus outgroups listed in Supplementary Data Table S1, which also provides information on vouchers, DNA loci sequenced and GenBank accession numbers. Seventy-nine sequences were newly generated for this study. The taxon sample covers all but one genus of the Areae [*Arum*, *Biarum*, *Dracunculus*, *Helicodiceros*, Australian *Typhonium* (= *Lazarum*), *Sauromatum*, *Theriophonum* and *Typhonium*]. Only *Eminium* is not included due to lack of chromosome counts. As outgroups, we used a species of *Alocasia*, 24 of *Arisaema* (one with two accessions) and five of *Pinellia*. Only species with known chromosome numbers are included. *Typhonium* itself is represented by 22 of its 50–60 species (one species is represented by two accessions).

To infer phylogenetic relationships, we relied on part of the nuclear phytochrome C gene (*PhyC*) and two chloroplast loci, the *rpl20–rps12* intergenic spacer and part of the lysine tRNA gene (*trnK*), which contains the maturase K intron (*matK*). Total DNA from silica-dried leaves was extracted with the NucleoSpin Plant II kit according to the manufacturer's protocol (Macherey-Nagel, Düren, Germany). Amplification and sequencing were performed using the primers described in Cusimano *et al.* (2010). Polymerase chain reactions were performed using 1·25 U of *Taq* DNA polymerase (New England Biolabs GmbH, Frankfurt am Main, Germany) and the following cycle conditions: the initial step of 3 min at 94 °C was followed by 39 cycles of 94 °C for 30 s for DNA denaturation, 54 °C for 60 s for primer annealing, 68 °C for 90 s for primer extension and 68 °C for 10 min after the final cycle. The PCR products were purified with Exo I and FastAP (Fermentas, St Leon-Rot, Germany). Sequencing was done on an ABI 3130-4 capillary sequencer, and sequences were assembled and edited with Sequencher 4·2 (Gene Codes Cooperation, Ann Arbor, MI, USA). All contigs were BLAST-searched in GenBank, which for nuclear sequences provides a check against fungal contamination and for plastid sequences a check against DNA from leaf epiphytes.

Phylogenetic analyses

Alignments were generated in MAFFT (http://mafft.cbrc.jp/alignment/server/) and checked visually using MEGA5 (Tamura *et al.*, 2011). To remove poorly aligned positions, single alignments were exported to a server running Gblocks vs. 0·91b (http://molevol.cmima.csic.es/castresana/Gblocks_server.html) with the less stringent options selected (Castresana, 2000). The plastid and nuclear data were first analysed separately and, in the absence of statistically supported topological contradictions ($>80 \%$), they were combined. The combined matrix (4252 aligned nucleotides) was used for maximum likelihood (ML) tree searches in RAxML (Stamatakis, 2006; Stamatakis *et al.*, 2008), using the GTR + G substitution model with four rate categories. Bootstrapping under ML used 1000 replicates. We also generated ultrametric trees in BEAST v. 1.7.5 (Drummond and Rambaut, 2007), using the same substitution model and a pure-birth Yule model as the tree prior. The analysis was run for 10 million generations, sampling every 1000th step. The burn-in fraction, i.e. the number of trees to be discarded from the consensus tree (the maximum clade credibility tree), was assessed using Tracer v. 1.4.1, which is part of the BEAST package.

Inference of chromosome number change

To infer ancestral haploid chromosome numbers, we relied on ChromEvol v. 1.3 of Mayrose *et al.* (2010). This lets users chose among eight models of chromosome number change that have the following six parameters: polyploidization (chromosome number duplication) with rate ρ, demi-polyploidization (polyploids derived from the fusion of gametes with different ploidy levels) with rate μ, and dysploidization (ascending, chromosome gain rate λ; descending, chromosome loss rate δ) as well as two linear rate parameters, λ_1 and δ_1, for the dysploidization rates λ and δ, allowing them to depend on the current number of chromosomes. Four of the models have a constant rate, whereas the other four include the two linear rate parameters. Both model sets also have a null model that assumes no polyploidization events. We fitted all models to the data, using either an ML phylogram or an ultrametric BEAST maximum clade probability tree, in each case with 10 000 simulated repetitions to compute the expected number of changes of the four transition types along each branch of the phylogeny. The maximum number of chromosomes was set to 10-fold higher than the highest number found in the empirical data, and the minimum number was set to 1. The root node was fixed to $a = 14$, based on our previous family-wide analysis (Cusimano *et al.*, 2012*a*).

Model fit was assessed using the Akaike information criterion (AIC). Mayrose *et al.* (2010) have shown that accurate reconstructions of ancestral chromosome numbers and events are only obtained from trees with intermediate evolutionary distances. We therefore adjusted the phylogram and ultrametric tree such that both had a total length of 0·2, which could be achieved by multiplying all branch lengths by suitable factors. Results were plotted in R using the ChromEvol functions version 0.9-1 of N. Cusimano (http://www.sysbot.biologie.uni-muenchen.de/en/people/cusimano/use_r.html).

Chromosome preparation, FISH analyses, DNA probes and C-banding

Bulbs of *Typhonium* were cultivated in the greenhouses of the Munich Botanical Garden, and, for most, plenty of root tips were available although usually only from a single individual. They originally came from W. Hetterscheid's taxonomic studies on *Typhonium* (Hetterscheid and Boyce, 2000; Hetterscheid and Nguyen, 2001; Hetterscheid *et al.*, 2001; Hetterscheid and Galloway, 2006; Hetterscheid, 2013). The chromosomes of 15 species (single individuals) were newly counted, namely *T. circinnatum*, *T. corrugatum*, *T. echinulatum*, *T. filiforme*, *T. gallowayi*, *T. huense*, *T. laoticum*, *T.* spec. H.AR. 664 (morphologically similar to *T. laoticum*, but clearly a separate species based on the molecular results), *T. orbifolium*, *T. saraburiense*, *T. stigmatilobatum*, *T. tubispathum*, *T. violifolium*, *Typhonium* spec. 17 Thailand, and *T. trilobatum*. Authors of species names and voucher material for each species are given in Supplementary Data Table S1.

Root tips were pre-treated in 2 mM 8-hydroxyquinoline for 20 h at 4 °C, fixed in freshly prepared 3:1 (v/v) ethanol/glacial acetic acid at room temperature overnight and kept at −20 °C. For chromosome preparations, fixed root tips were washed three times for 5 min in distilled water, digested with 1 % cellulase (w/v; Onozuka RS, Serva), 0·4 % pectolyase (w/v; Sigma), 0·4 % cytohelicase (w/v; Sigma) in citric buffer, pH 4·8 for 30 min at 37 °C, dissected in a drop of 45 % acetic acid and squashed. Coverslips were removed after freezing in dry ice, and preparations were air-dried at room temperature. The quality of spreads was checked microscopically using phase contrast, and only preparations with at least ten well-spread metaphases were used for FISH. For *T. filiforme*, *T. gallowayi*, *T. orbifolium*, *T. tubispathum* and *Typhonium* spec. 17 Thailand, only a few cells per species (1–5) were counted. Pictures were taken using 4',6-diamidino-2-phenylindole (DAPI) staining (*T.* spec. 17 Thailand) and without staining using a phase contrast microscope.

We performed FISH with a telomeric probe, and 5S rDNA and 45S rDNA probes; the telomeric probe was not used on *T. violifolium* because of a shortage of suitable material. To locate rDNAs, we used the 18S−5·8S−25S rDNA repeat unit of *Arabidopsis thaliana* in the pBSK+ plasmid, labelled with digoxigenin-11-dUTP (Roche) by nick translation, and a 349 bp fragment of the 5S rRNA gene repeated unit from *Beta vulgaris* cloned into pBSK+ (Schmidt *et al.*, 1994), labelled with biotin-16-dUTP (Roche) by PCR. The *Arabidopsis*-like telomeric probe was amplified by PCR according to Ijdo *et al.* (1991) using the oligomer primers (5′-TTTAGGG-3′)$_5$ and (5′-CCCTAAA-3′)$_5$, and labelled with digoxigenin-11-dUTP

TABLE 1. *Inferred chromosome number evolution in the Areae and their immediate outgroups under the best-fitting model, the linear-rates model with the duplication (polyploidzation) rate different from the demi-duplication rate*

Tree	Factor	Total tree length	Root tip length	Best model	LogLik	AIC	Rates				Number of events				
							λ	δ	ρ	μ	Gains	Losses	Duplications	Demi.	Total events
Ultrametric	4·5	3·5	0·045	lrde	−262·3	536·5	0·33	15·21	10·39	2·23	6·5	31·1	33·4	5	76
Phylogram	5	2·1	0·04	crde	−329·2	666·4	1·78	22·9	17·26	4·26	2·5	38·3	31·2	8·9	80·9

Column two refers to the factor used to multiply branch lengths to obtain a suitable root to tip length for the tree (see the Materials and Methods); columns three and four give the lengths obtained after adjusting branch lengths by the multiplication factor; column five gives the logarithmic likelihood; column six gives the AIC scores to the likelihood ratio tests.

The symbols for the rates inferred for all events in the tree are λ, chromosome gain rate; δ, chromosome loss rate; ρ, duplication rate; μ, demi-duplication rate.

The number of events refers to the four event types with an expectation >0·5 (demi., demi-duplication).

The last column shows the total number of events inferred on the respective tree.

by nick translation. Hybridization mixes consisted of 50 % formamide (w/v), 2× SSC, 10 % dextran sulfate (w/v) and 70–200 ng of labelled probe. The hybridization mix was denatured at 75 °C for 10 min and immediately cooled on ice for 10 min; 10–15 μL of the mix was then added to each slide. Hybridization was carried out in a humid chamber at 37 °C for 20 h. The 5S rDNA was detected with streptavidin–Cy3 conjugate (Sigma), and the 45S rDNA with anti-digoxigenin–fluorescein isothiocyanate (FITC) conjugate (Roche) at 37 °C for 1 h. The chromosomes were counterstained with DAPI (2 μg mL^{-1}) and mounted in Vectashield (Vector). Slides first analysed with telomeric and 5S rDNA probes were de-stained, and a second hybridization was performed with 45S rDNA to obtain a sequential staining with both markers in a single cell. For more details, see Sousa *et al.* (2013).

To study a supernumerary chromosome discovered in *T. trilobatum*, we performed C-banding and FISH using the nuclear ribosomal internal transcribed spacer 2 (ITS2) of this species. The ITS2 of *T. trilobatum* was amplified by PCR using primers ITS3 and ITS4 (White *et al.*, 1990). The resulting DNA fragment (KC478077) was cloned into the pGEM-T Easy plasmid (Promega, Mannheim, Germany), sequenced and PCR-labelled with biotin-16-dUTP (Roche). Procedures for chromosome preparation, post-hybridization washes and C-banding follow Sousa *et al.* (2013).

Images were taken with a Leica DMR microscope equipped with a KAPPA-CCD camera and the KAPPA software. They were optimized for optimum contrast and brightness using Adobe Photoshop CS3 version 10.0.

RESULTS

New chromosome counts for 15 Typhonium *species*

The new chromosome counts for 15 *Typhonium* species range from $2n = 8$, the lowest number reported so far for the Araceae family, to $2n = 24$ (Table 2). Of the 15 species, five displayed odd chromosome numbers. Prior to our study, an aneuploid number, namely $2n = 65$, had only been reported for *T. roxburghii* (as *T. divaricatum*) (Ramachandran, 1978), but in other genera, such as *Amorphophallus*, *Anthurium*, *Apoballis*, *Arisaema*, *Arum*, *Caladium*, *Pinellia* and *Schismatoglottis*, aneuploidy is well documented (Cusimano *et al.*, 2012a). For *Anthurium* and *Schismatoglottis*, the aneuploid numbers have been discussed as possible B chromosomes (Cusimano *et al.*, 2012a).

Ancestral state reconstructions for Typhonium chromosome numbers

The combined matrix of nuclear and chloroplast markers (96 species and subspecies, 22 of them *Typhonium*; 4252 nucleotides) yielded a well-supported phylogeny (Fig. 1). We then used either the ML phylogram or an ultrametric tree (see the Materials and Methods), and chromosome counts for all 96 accessions, to model chromosome evolution, fitting all models implemented in the ChromEvol program and comparing their likelihood using AIC scores. A reconstruction on an ultrametric tree is shown in Fig. 1 and a reconstruction on a phylogram is shown in Supplementary Data Fig. S1. The statistical support for both is shown in Supplementary Data Figs S2 and S3. The best-fitting models differ slightly, depending on the tree's overall branch lengths, which is their only difference, and is shorter in the phylogram than in the ultrametric tree (phylogram 2·1 vs. ultrametric tree 3·5; Table 1). On the phylogram, the four-parameter-constant-rate model, which assumes constant gain and loss rates and a polyploidization rate that differs from the demi-polyploidization rate, best explained the empirical numbers at the tips of the tree (AIC = 666·2). On the ultrametric tree, the six-parameter-linear-rate model, which includes additional parameters for the gain and loss rates (making them linearly dependent on the current chromosome number), best explained the empirical data (AIC = 536·5). The inferred rates of change and numbers of events on the two trees are summarized in Table 1.

TABLE 2. Typhonium *species investigated with their chromosome number, presence of interstitial telomeric signals (*Its*) and distribution of 5S and 45S rDNA sites*

Species	$2n$	*Its*	No.	5S rDNA	No.	45S rDNA
Typhonium circinnatum	24	–	1	Sub-terminal	8	Interstitial/terminal
T. violifolium	22	–	1	Sub-terminal	2	Terminal
T. corrugatum	20	–	1	Interstitial	2	Terminal
T. trilobatum	19	–	1	Sub-terminal	2	Terminal
T. saraburiense	18	–	1	Sub-terminal	2	Terminal
T. echinulatum	18	–	1	Sub-terminal	2	Terminal
T. huense	15	–	1	Interstitial	**2**	Terminal
T. stigmatilobatum	15	–	1	Interstitial	**2**	Terminal
T. laoticum	9	2	1	Proximal	1	Terminal
T. spec. H.AR. 664	8	5	1	Interstitial	2	Terminal
*T. filiforme**	12	–	–	–	–	–
*T. gallowayi**	20	–	–	–	–	–
*T. orbifolium**	12	–	–	–	–	–
T. spec. 17 Thailand*	19	–	–	–	–	–
*T. tubispathum**	10	–	–	–	–	–

Authors of species names and voucher information are given in Supplementary Data Table S1.
An asterisk marks species for which only chromosome counts were obtained.
Atypical numbers of 45S rDNA sites (five instead of four) are shown in bold.
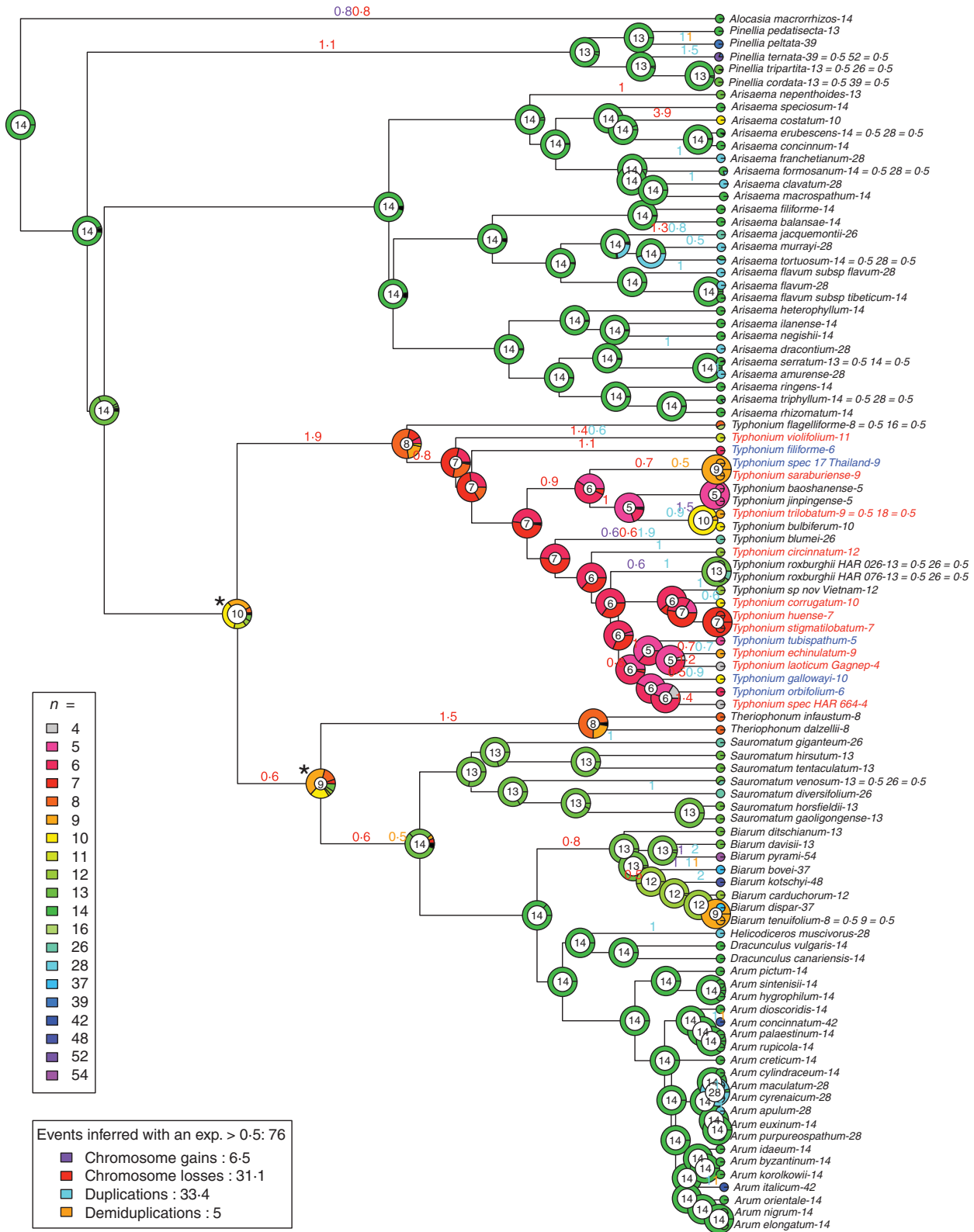
Fig. 1. Chromosome number reconstruction for the Areae on an ultrametric tree, rooted on *Alocasia macrorrhizos*. Pie charts represent the probabilities of inferred numbers, with the number inside a pie having the highest probability. Numbers above branches are colour coded by event type (gains, losses, duplications and demi-duplication) as shown in the rectangular inset, and represent the frequency with which an event type(s) with a probability >0·5 occurred along a branch. The colour coding of chromosome numbers is explained in the elongate inset on the left. Problematic inferences on the backbone are marked with an asterisk. Species investigated by FISH are labelled in red; species with only chromosome counts are labelled in blue.

The inferred chromosome gains, losses, duplication (polyploidization) and demi-duplications are shown in the insets in the lower left of Fig. 1, and Supplementary Data Figs S1 and S3. The number of events with an expectation >0·5 is similar on the phylogram and the ultrametric tree (80·6 vs. 76; Table 1). The predominant events were chromosome losses and duplications (31·1 vs. 33·4 on the ultrametric tree), with the number of inferred losses being slightly higher on the phylogram (38·3). There are few inferred chromosome gains (phylogram 2·5; ultrametric tree 6·5) and demi-duplications (phylogram 8·9; ultrametric tree 5).

Inferred ancestral haploid chromosome numbers, which we refer to as a, are shown in the pie diagrams at the nodes of the trees. They were similar on the phylogram and ultrametric tree, with a few exceptions, mostly at deeper internal nodes where inferences had low statistical support [posterior probability (PP) <0·4; see legend in Fig. 1 and Supplementary Data Fig. S1]. Inference on the backbone was problematic for two nodes (marked with an asterisk in Fig. 1 and Supplementary Data Fig. S1) involving *Typhonium*, and *Theriophonum* for which an ancestral number of $a = 8$ has been inferred. These genera are embedded in clades with $a = 14$, which results in an inferred (but not statistically supported) decrease from $a = 14$ via 10 and 9, back to 14. Along the *Typhonium* backbone, the inferred ancestral haploid numbers decrease from $a = 8$ to 7, 6 and 5, with different states inferred for nodes in the *T. saraburiense/ T. bulbiferum* clade on the phylogram and ultrametric tree (Fig. 1; Supplementary Data Fig. S1): on the ultrametric tree the inferred ancestral number for this clade is $a = 6$ (5) with the higher numbers ($n = 9, 10$) deriving from polyploidization events, and $n = 5$ in *T. baoshanense* and *T. jingpigense* being the ancestral condition. On the phylogram, the ancestral number is inferred as $a = 10$, with $n = 5$ the consequence of several chromosome losses. On both trees, other higher numbers, such as $n = 12$ in *T. circinnatum*, $n = 13$ in *T. roxburghii* and $n = 26$ in *T. blumei*, are inferred as resulting from polyploidization, while low numbers, such as $n = 4$ in *T.* spec. H.AR. 664 and in *T. laoticum*, are inferred as resulting from chromosome losses (descending dysploidy). Compared with the remaining Areae and the clade's outgroups, *Typhonium* has a low ancestral number ($a = 8$ or 7).

Molecular cytogenetic results

Observed chromosome numbers of the ten FISH-investigated species of *Typhonium* range from $2n = 8$ to $2n = 24$ (Table 2). They all have only one 5S rDNA site, with its distribution varying between species. In four species it was located interstitially, in five sub-terminally and in *T. laoticum* it had a proximal position (Figs 2 and 3B, E, H, K, N; Table 2). Most species had two 45S rDNA sites, predominantly distributed in terminal regions (Figs 2F, I, L, O and 3C, O). *Typhonium laoticum* ($2n = 9$) had a single 45S rDNA site, localized terminally on a chromosome pair (Fig. 3L), and *T. circinnatum* ($2n = 24$) had eight 45S rDNA sites located interstitially and/or terminally in eight chromosome pairs (Fig. 2C). *Typhonium huense* and *T. stigmatilobatum*, both with $2n = 15$, each had two 45S rDNA sites with an unusual number of signals (five; Fig. 3F, I; Table 2). The 5S and 45S rDNA sites were distributed on different chromosomes, with the exception of *T. circinnatum*,

T. huense and *T. stigmatilobatum* (Figs 2B, C and 3E, F, H, I). rDNA satellites were seen in most cells (Figs 2L, O and 3F, L, O). For species on which no FISH experiments were performed, pictures of mitotic metaphases are provided in Supplementary Data Fig. S4.

Telomeric signals were localized at chromosome ends in all species. *Typhonium laoticum* in addition had two *Its* on its largest chromosome pair (Fig. 3J), and *Typhonium* spec. H.AR. 664 ($2n = 8$) had five *Its* positioned close to terminal regions on five chromosomes (Fig. 3M).

One small chromosome of the aneuploid species *T. trilobatum* (Fig. 2L, white arrowhead) yielded a diffuse rDNA signal, so we undertook additional experiments to find out the heterochromatin composition of this chromosome and if the diffuse 45S rDNA signal might be related to the amplification of one of its internal transcribed spacers. Similar experiments have been performed in plant species with B chromosomes (Dhar *et al.*, 2002; Marschner *et al.*, 2007). With C-banding (Fig. 4A, B), one chromosome was labelled along its length and was thus heterochromatic (Fig. 4B), while other chromosomes were labelled in sub-terminal or terminal regions. A *T. trilobatum*-specific ITS2 probe revealed only four signals (Fig. 4D) distributed in sub-terminal/terminal regions of a large and medium chromosome pairs. These sites represent the two rDNA sites seen in Fig. 2L.

DISCUSSION

Phylogenetic modelling of chromosome number change

With the current sampling of *Typhonium* (22 of its 50–60 species are included in our phylogeny) it appears that low chromosome numbers evolved twice, once in *T. baoshanense* and *T. jinpingense*, both with $2n = 10$ (Zhonglang *et al.*, 2002; Zhin-Lin *et al.*, 2007) and embedded among species with $2n = 18$–20, and again in *T. tubispathum* ($2n = 10$), *T. laoticum* ($2n = 9$) and *T.* spec. H.AR. 664 ($2n = 8$), which are embedded among species with $2n = 12, 18$ or 20. We believe that this inference is reliable because the tree is robust (nuclear and plastid regions were used; relevant nodes have good statistical support), and the key finding of a high dysploidy rate is insensitive to whether the inferences were made on a phylogram or on an ultrametric tree. How exactly branch lengths influence chromosome number reconstruction is currently not understood, and it is advisable to carry out maximum likelihood runs on both types of trees and then to trust those findings supported by both sets of reconstructions (Cusimano and Renner, 2014). Clearly, all character state reconstruction also stands and falls with dense species sampling and reliable counts for the included species. Regarding species sampling and chromosome counts in *Typhonium*, we have data for only about half the species in the genus. If the missing species had generally higher numbers, the inferred ancestral number in *Typhonium* might increase. However, the conclusion of at least two independent dysploidy events will not change by an improved sampling.

The main purpose of placing chromosome numbers in a phylogenetic context is to infer the likely direction of change, from high to low numbers or the other way around. While this is difficult to achieve, having an evolutionary framework is essential. Only cytogenetic methods, however, can then lead to an understanding of the mechanisms behind any inferred changes, and
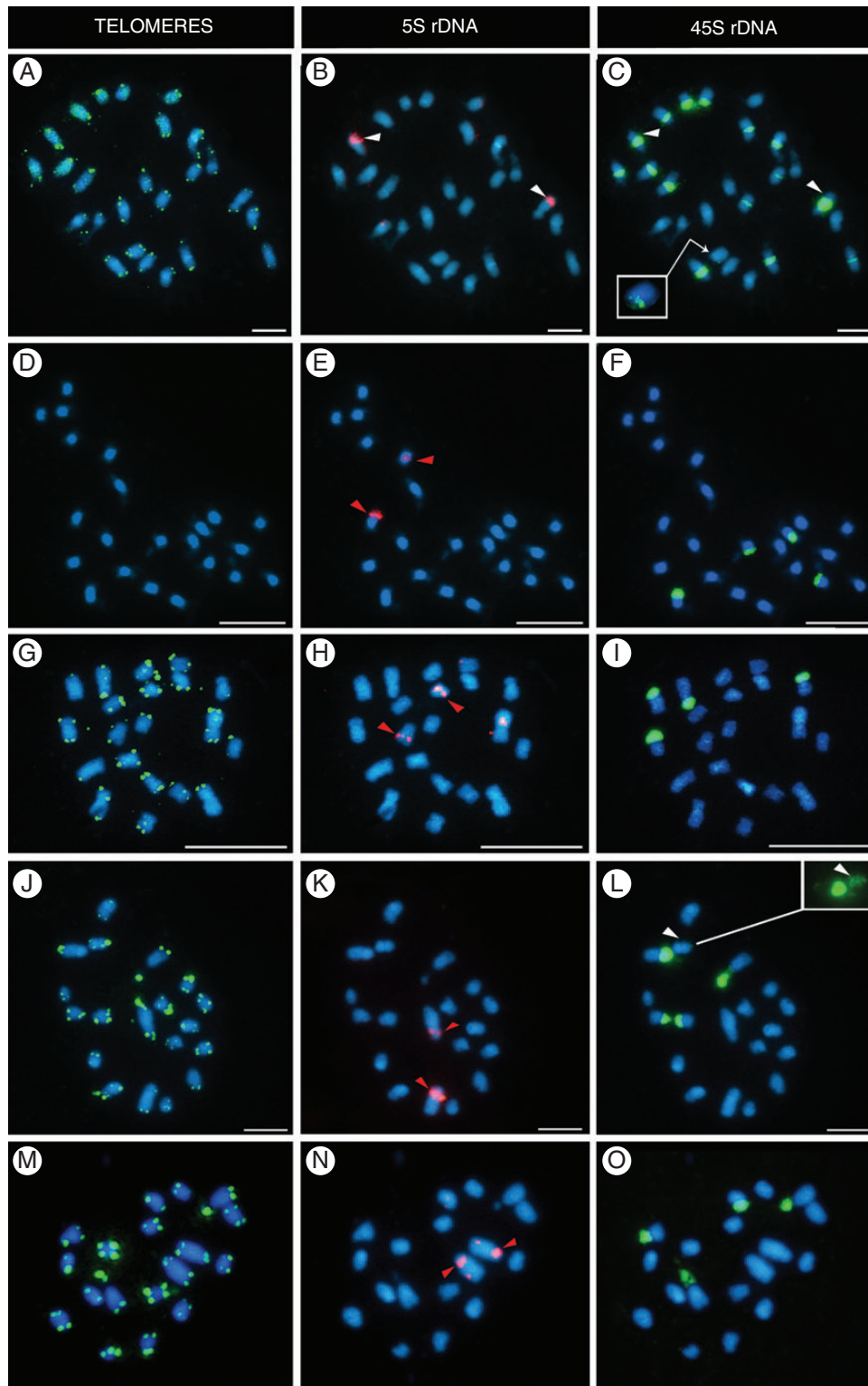
FIG. 2. Detection of telomeric signals, 5S and 45S rDNA sites in chromosomes of (A–C) *Typhonium circinnatum* ($2n = 24$), (D–F) *T. violifolium* ($2n = 22$), (G–I) *T. corrugatum* ($2n = 20$), (J–L) *T. trilobatum* ($2n = 19$) and (M–O) *T. saraburiense* ($2n = 18$) by FISH. Red arrowheads indicate the position of 5S rDNA sites in all cells, whereas white arrowheads in B and C indicate a chromosome pair with both rDNA sites, and in L a chromosome exhibiting a dispersed 45S rDNA signal. Insets in C show a chromosome with a weak 45S rDNA treated with a differential brightness/contrast, and in L a fifth diffuse 45S rDNA signal that overlaps the supernumerary chromosome. Scale bars = 5 μm.
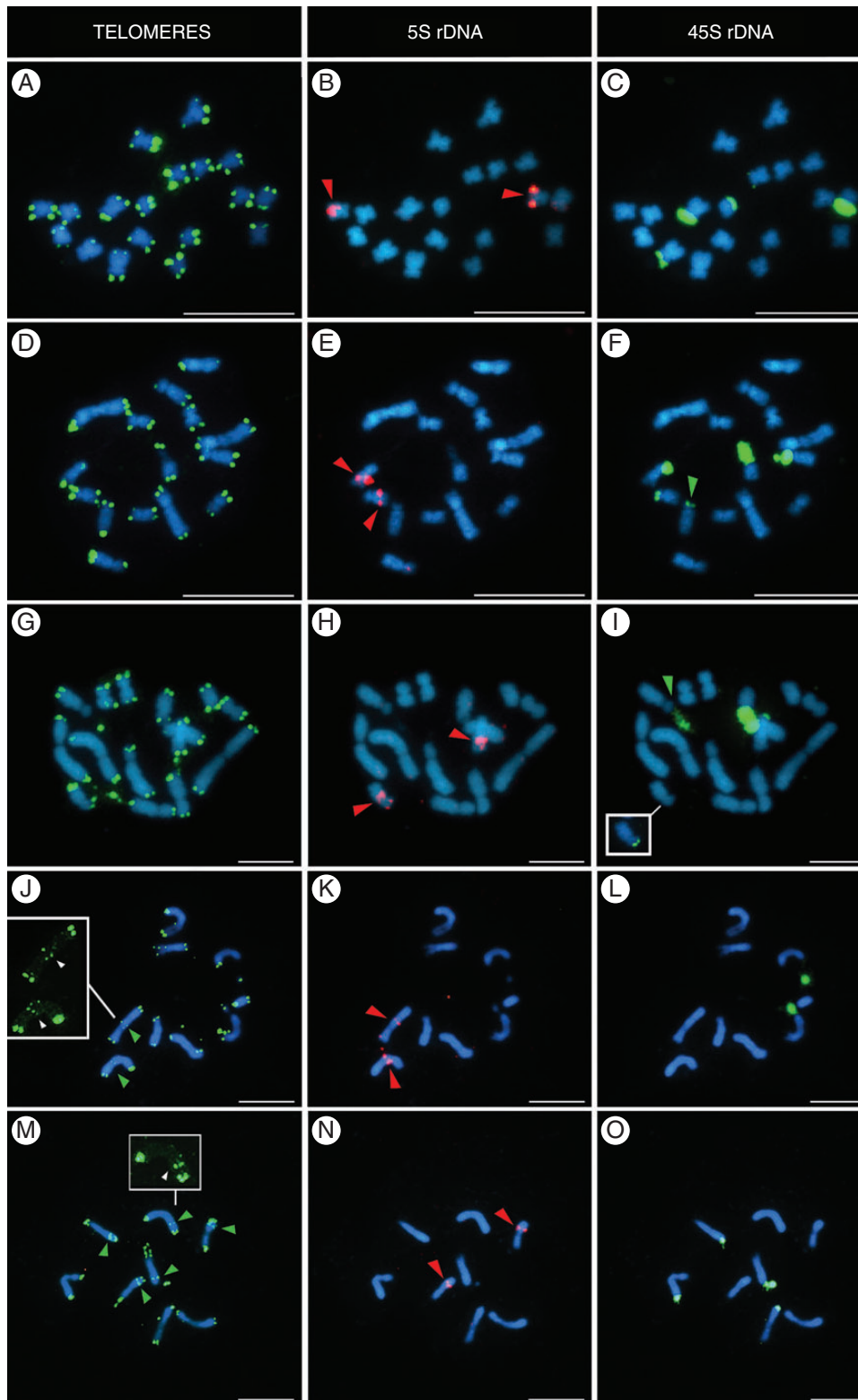
F𝐼𝐺. 3. Detection of telomeric signals, 5S and 45S rDNA sites in chromosomes of (A–C) *Typhonium echinulatum* ($2n = 18$), (D–F) *T. huense* ($2n = 15$), (G–I) *T. stigmatilobatum* ($2n = 15$), (J–L) *T. laoticum* ($2n = 9$) and (M–O) *T.* spec. H.AR. 664 ($2n = 8$) by FISH. Red arrowheads indicate the position of 5S rDNA sites in all cells, while green arrowheads in F and I indicate a fifth 45S rDNA signal and in J and M interstitial telomeric signals. Insets in I show chromosome with a weak 45S rDNA signal treated with a differential brightness/contrast, and in J and M display chromosomes with the telomeric probe, without the overlapping with DAPI. Scale bars = 5 μm.
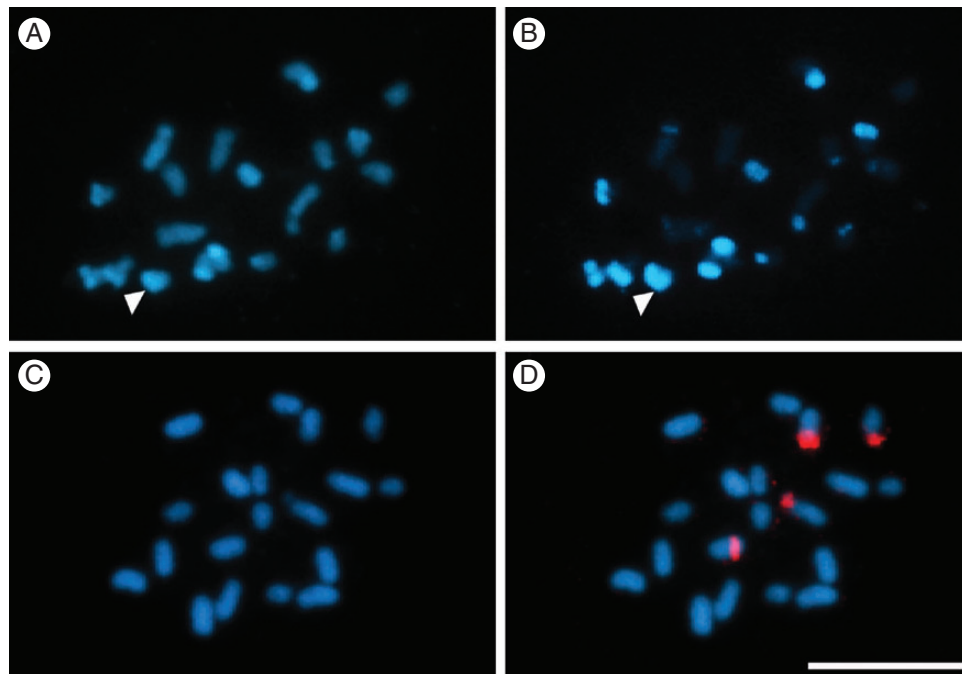
FIG. 4. Karyograms of *Typhonium trilobatum* (2*n* = 19). (A) Metaphase before and in (B) after C-banding. The heterochromatin is restricted mainly to sub-terminal/terminal regions of chromosomes, but only one chromosome (white arrowhead) was completely labelled and thus is heterochromatic. (C) Metaphase stained only with DAPI, and in (D) four signals visible after application of the *T. trilobatum* ITS2 probe. These signals correspond to the two sites of 45S rDNA. Scale bars = 5 μm.

full genome sequencing is required for detailed synteny. In this study, we brought together several of these approaches, using the same plant accessions, because we were initially critical of the high rate of chromosome 'loss' (decreasing dysploidy) inferred by the modelling approach.

Testing some of the inferred events with FISH

The FISH experiments, which to our knowledge are the first in the Araceae, revealed *Its* in the two *Typhonium* species with the lowest chromosome numbers, *T. laoticum* and *T.* spec. H.AR. 664. The ancestral state reconstructions (Fig. 1; Supplementary Data Fig. S1) for these species suggested number reduction by descending dysploidy. In other species with relatively low numbers, such as *T. stigmatilobatum* and *T. huense*, no dysploidy was inferred and no *Its* were detected. The cytogenetic evidence of *Its*, low chromosome numbers (incidentally including the lowest in the family) and aneuploid number series in combination suggests that dysploidy is an important mechanism in *Typhonium*. The consequences of dysploidy may include karyotype asymmetry and possibly also B chromosomes (Raskina *et al.*, 2008). Aneuploid numbers probably originate through meiotic irregularities leading to the formation of aneuploid gametes. Our *Typhonium* bulbs had been maintained in cultivation for several years, and, for each species, we had only one or a few individuals available for counting. Thus, the aneuploid chromosome numbers reported here may not represent the natural condition. It is also possible that some of the species are polyploids, suffering meiotic irregularities. So far, polyploidy had only been inferred for *T. trilobatum* and *T. roxburghii* (Cusimano *et al.*, 2012a; Supplementary Data Table S1), and we newly inferred it for *T. circinnatum* (see below).

How trustworthy are *Its* as indicators of evolutionary chromosome rearrangements (fusions) in *Typhonium*? Normally, telomeres protect chromosomes from end to end fusion (Slijepcevic, 1998), and their (rare) location in interstitial chromosome regions revealed in FISH studies is therefore interesting. Supplementary Data Fig. S5 illustrates the explanations proposed so far. Interstitial telomere signals have been related to paracentric or pericentric inversions, processes that do not imply a reduction in chromosome number (Supplementary Data Fig. S5a modified from Schubert, 2007). Another explanation for them is chromosome fusion by symmetrical reciprocal translocation involving the centromere (Supplementary Data Fig. S5b modified from Schubert and Lysak, 2011). This gives rise to a single chromosome and a small fragment composed mainly of the centromere of one chromosome and short rests of both previous chromosomes and their telomeres. Such short fragments will be eliminated from the cell unless they carry essential genes. A third mechanism, called a fusion–fission cycle or Robertsonian rearrangement, involves a reciprocal translocation with breakpoints within the telomeric arrays of two telocentric chromosomes. This preserves both chromosomes' centromeres and telomere sequences although one of the centromeres and the interstitial telomeric sequences must be inactive (Schubert and Lysak, 2011; Supplementary Data Fig. S5c). A large dicentric chromosome with/without *Its* may result, which can then break again and form two viable telocentric chromosomes (after formation of new telomeres). In plants, fusion–fission cycles have been documented in *Vicia faba* (Schubert *et al.*, 1995; Fuchs *et al.*, 1995: fig. 1). In *T. laoticum* and *T.* spec. H.AR. 664, however, we observed only one primary constriction, not two, which does not fit with a classical Robertsonian rearrangement.

To explain the *Its* localized in the proximal region of the largest chromosome pair of *T. laoticum*, we now propose a new explanation (Fig. 5). It assumes a reciprocal translocation between two acrocentric chromosomes, with one chromosome having breaks in its telomere sequence array and the other having breaks close to the centromeric region of its long arm. The product of this translocation would be a submetacentric chromosome with a weakly detectible *Its*, no longer functional, plus a small chromosome comprising only part of the telomere sequence from one donor and the entire short arm and centromere of the other donor. Alternatively, a metacentric chromosome would be formed plus a small DNA fragment composed by only part of a telomere sequence from one donor and a centromere and complete telomere sequence array from the other donor (Fig. 5). We never found such small chromosomes, but the co-localization of *Its* with rDNA is suggestive. The presence of two *Its* in the proximal region of a large chromosome in *Sideritis montana* (2*n* = 16) has also been interpreted as indicating centric fusion and adduced to explain descending dysploidy (Raskina *et al.*, 2008).

To explain the *Its* close to the terminal regions of five chromosomes in *Typhonium* spec. H.AR. 664, we assume a mechanism similar to what has been suggested for *Pinus* (Schmidt *et al.*, 2000). Telomere-like repeats are highly amplified in *Pinus elliottii* and not restricted to the ends of chromosomes; instead they form large intercalary and pericentric blocks, attributed to random short sequence arrays, perhaps extended by slippage replication, insertion of extrachromosomal linear DNA fragments, or inversions (Biessmann and Mason, 1992). Meiotic studies would further clarify the pathways by which *T.* spec. H.AR. 664 (and also *T. laoticum*) acquired their low chromosome numbers. For example, a chromosome ring, as seen in *Eleocharis subarticulata* in meiosis I (Da Silva *et al.*, 2005), would point to multiple translocations having played a role in the reduction of chromosome number.

Polyploidy in T. circinnatum, *loss of a chromosome pair in* T. laoticum *and an rDNA cluster jump or amplification in* T. huense, T. stigmatilobatum *and* T. circinnatum
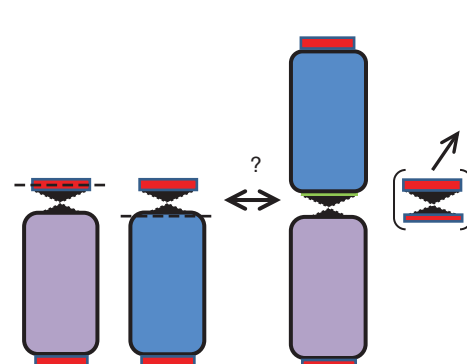
The 45S rDNA sites in *Typhonium* are stable in number and position (Table 2). Eight of the ten investigated species have two 45S rDNA sites, although *T. huense* and *T. stigmatilobatum* showed five instead of four signals at the two sites. Only *T. laoticum* has one site and *T. circinnatum* has eight rDNA
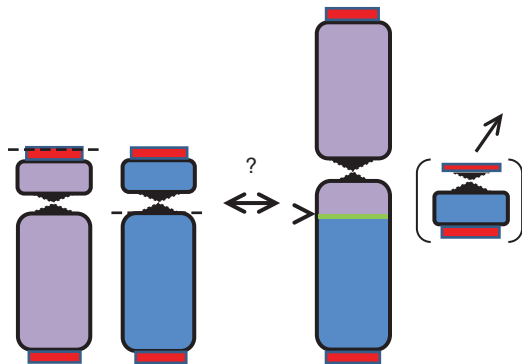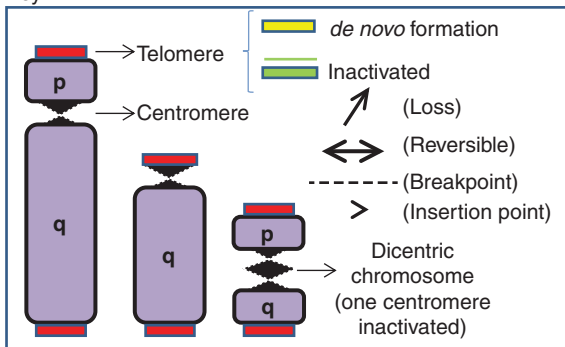

FIG. 5. Mechanisms explaining the interstitial telomeric signals on chromosomes of *Typhonium laoticum* (see text for details). Chromosome arms are labelled p for the short arm and q for the long arm. Telocentric chromosomes present only the long arm.

sites. The increase of rDNA sites might indicate polyploidization, as indeed suggested by our chromosome number reconstruction for *T. circinnatum* (Fig. 1; Supplementary Data Fig. S1). Known polyploid angiosperms commonly show increased numbers of rDNA sites. Thus, in *Trifolium*, the allotetraploid *T. dubium* has twice the number the rDNA sites compared with any of its diploid parents, indicating additive inheritance (Ansari *et al.*, 2008). Also in *Aloe*, rDNA inheritance in polyploids is sometimes additive (Adams *et al.*, 2000). However, in the allotetraploid *Tragopogon mirus* and *T. miscellus*, both with $2n = 24$, the copy numbers of rDNA sites are slightly less than double the parental numbers (Kovarik *et al.*, 2005), while in intraspecific polyploids in *Passiflora*, rDNA site numbers exceed those expected under additive inheritance (De Melo and Guerra, 2003). Based on these examples, the eight rDNA sites of *Typhonium circinnatum* may well indicate a polyploidization event. Alternative explanations involve jumping nucleolus-oganizing regions (Schubert and Wobus, 1985; for a review, see Raskina *et al.*, 2008), perhaps mediated by transposable elements. Such events could also explain the odd numbers of rDNA signals in *T. huense* (Fig. 3D–F) and *T. stigmatilobatum* (Fig. 3G–I). For *T. laoticum* (Fig. 3J–L), the loss of one chromosome pair with its rDNA site may explain the species' single 45S rDNA site.

B chromosomes in the Araceae – insufficiently tested so far

Supernumerary or putative B chromosomes have been reported from numerous species in seven genera of Araceae (*Anthurium*, *Apoballis*, *Arisaema*, *Asterostigma lividium*, *Philodendron radiatum*, *Piptospatha burbidgei* and *Schismatoglottis*), although not from *Typhonium* (original references in Supplementary Data table S1 in Cusimano *et al.*, 2012a). None of these studies used meiotic analyses for a more detailed understanding. Our C-banding and FISH experiments (using a specific ITS2 probe from *T. trilobatum*; Fig. 4A–D) appear to be the first molecular–cytogenetic analyses of any aneuploid chromosome number in the Araceae. The C-banding showed that heterochromatin blocks were mainly distributed in terminal regions of the regular chromosomes, while at least one small chromosome was completely stained (Fig. 4B). The complete staining resembles the situation in *Plantago lagopus* B chromosomes (Dhar *et al.*, 2002), a species in which the repetitive DNA of B chromosomes consists mainly of 5S rDNA (as shown with FISH). The small heterochromatic chromosome of *T. trilobatum* instead contained a single diffuse 45S rDNA signal (Fig. 2L, inset). Using the 18S nuclear ribosomal ITS2 of *T. trilobatum* as an *in situ* hybridization probe, we detected only four signals (Fig. 4D), representing the typical two 45S rDNA sites (Fig. 2L). These experiments, of course, are insufficient to establish the presence of B chromosomes, which can only be done by demonstrating meiotic drive in a population.

Conclusions

The new cytogenetic data supported two model-based inferences of descending dysploidy and one of polyploidization obtained in phylogenetic reconstructions of chromosome number change along a molecular phylogeny for *Typhonium* (using both phylograms and ultrametric trees). This is the first time that phylogenetic trait reconstruction for chromosome numbers has been tested by physical (microscopy-based) evidence. We also provide a detailed cytogenetic investigation of the aneuploid karyotype of *T. trilobatum*. The heterochromatic constitution of one of this species' chromosomes and the detection of dispersed 45S rDNA signals are reminiscent of B chromosomes in other plant species. However, without meiotic analyses, the existence of B chromosomes in the Araceae remains speculative.

SUPPLEMENTARY DATA

Supplementary data are available online at www.aob.oxfordjournals.org and consist of the following. Table S1: species and DNA regions sequenced, their sources and GenBank accession numbers. Figure S1: chromosome number reconstruction for the Areae on a phylogram, rooted on *Alocasia macrorrhizos*. Figure S2: maximum likelihood phylogeny for the Areae and three outgroups (*Alocasia*, *Arisaema* and *Pinellia*) based on the combined analysis of plastid and nuclear markers (4252 aligned nucleotides). Figure S3: chromosome number reconstruction for the Areae on an ultrametric tree rooted on *Alocasia macrorrhizos*. Figure S4: mitotic metaphases of *Typhonium filiforme*, *T. orbifolium*, *T.* spec. 17 Thailand and *T. gallowayi*, and karyogram of *T. tubispathum*. Figure S5: chromosome rearrangements that may lead to a reduction of chromosome numbers.

LITERATURE CITED

Adams SP, Leitch IJ, Bennett MD, Chase MW, Leitch AR. 2000. Ribosomal DNA evolution and phylogeny in *Aloe* (Asphodelaceae). *American Journal of Botany* **87**: 1578–1583.

Ansari HA, Ellison NW, Williams WM. 2008. Molecular and cytogenetic evidence for an allotetraploid origin of *Trifolium dubium* (Leguminosae). *Chromosoma* **117**: 159–167.

Biessmann H, Mason JM. 1992. Genetics and molecular biology of telomeres. *Advances in Genetics* **30**: 185–249.

Boyce PB, Croat TB. 2013. *The Überlist of Araceae. Totals for published and estimated numbers of species in aroid genera* (http://www.aroid.org/genera/130307uberlist.pdf).

Castresana J. 2000. Selection of conserved blocks from multiple alignments for their use in phylogenetic analysis. *Molecular Biology and Evolution* **17**: 540–552.

Cusimano N, Renner SS. 2014. Further on the effects of branch lengths on ancestral state reconstruction. *Systematic Biology* (in press).

Cusimano N, Barrett M, Hetterscheid WLA, Renner SS. 2010. A phylogeny of the Areae (Araceae) implies that *Typhonium, Sauromatum* and the Australian species of *Typhonium* are distinct clades. *Taxon* **59**: 439–447.

Cusimano N, Bogner J, Mayo SJ, *et al*. 2011. Relationships within the Araceae: comparisons of morphological patterns with molecular phylogenies. *American Journal of Botany* **98**: 654–668.

Cusimano N, Sousa A, Renner SS. 2012a. Maximum likelihood inference implies a high, not a low, ancestral haploid chromosome number in the Araceae, with a critique of the bias introduced by 'x'. *Annals of Botany* **109**: 681–692.

Cusimano N, Stadler T, Renner SS. 2012b. A new method for handling missing species in diversification analysis applicable to randomly or non-randomly sampled phylogenies. *Systematic Biology* **61**: 785–792.

Da Silva CRM, González-Elizondo MS, Vanzela ALL. 2005. Reduction of chromosome number in *Eleocharis subarticulata* (Cyperaceae) by multiple translocations. *Botanical Journal of the Linnean Society* **149**: 457–464.

De Melo NF, Guerra M. 2003. Variability of 5S and 45S rDNA sites in *Passiflora* L. species with distinct base chromosome numbers. *Annals of Botany* **92**: 309–316.

Dhar MK, Friebe B, Koul AK, Gill BS. 2002. Origin of an apparent B chromosome by mutation, chromosome fragmentation and specific DNA sequence amplification. *Chromosoma* **111**: 332–340.

Drummond AJ, Rambaut A. 2007. Bayesian evolutionary analysis by sampling trees. *BMC Evolutionary Biology* **7**: 214.

Fuchs J, Brandes A, Schubert I. 1995. Telomere sequence localization and karyotype evolution in higher plants. *Plant Systematics and Evolution* **196**: 227–241.

Hetterscheid WLA. 2013. New *Typhonium* species from Asia. *Aroideana* **36**: 93–97.

Hetterscheid WLA, Boyce PC. 2000. A reclassification of *Sauromatum* Schott and new species of *Typhonium* Schott (Araceae). *Aroideana* **23**: 48–55.

Hetterscheid WLA, Galloway A. 2006. New *Typhonium* (Araceae) species from Thailand. *Aroideana* **29**: 80–85.

Hetterscheid WLA, Nguyen VD. 2001. Three new species of *Typhonium* (Araceae) from Vietnam. *Aroideana* **24**: 24 – 29.

Hetterscheid WLA, Sookchaloem D, Murata J. 2001. *Typhonium* (Araceae) of Thailand: new species and a revised key. *Aroideana* **24**: 30–55.

Ijdo JW, Wells RA, Baldini A, Reeders ST. 1991. Improved telomere detection using a telomere repeat probe (TTAGGG)n generated by PCR. *Nucleic Acids Research* **19**: 17.

Kovarik A, Pires JC, Leitch AR, *et al*. 2005. Rapid concerted evolution of nuclear ribosomal DNA in two *Tragopogon* allopolyploids of recent and recurrent origin. *Genetics* **169**: 931–944.

Larsen K. 1969. Cytology of vascular plants: III. A study of Aroids. *Dansk Botanisk Arkiv* **27**: 39–59.

Marchant CJ. 1973. Chromosome variation in Araceae IV: from Acoreae to Lasieae. *Kew Bulletin* **28**: 199–210.

Marschner S, Meister A, Blattner FR, Houben A. 2007. Evolution and function of B chromosome 45S rDNA sequences in *Brachycome dichromosomatica*. *Genome* **50**: 638–644.

Mayrose I, Barker MS, Otto SP. 2010. Probabilistic models of chromosome number evolution and the inference of polyploidy. *Systematic Biology* **59**: 132–144.

Nauheimer L, Boyce PC, Renner SS. 2012. Giant taro and its relatives: a phylogeny of the large genus *Alocasia* (Araceae) sheds light on Miocene floristic exchange in the Malesian region. *Molecular Phylogenetics and Evolution* **63**: 43–51.

Petersen G. 1993. Chromosome numbers of the genera of Araceae. *Aroideana* **16**: 37–46.

Ramachandran K. 1978. Cytological studies on South Indian Araceae. *Cytologia* **43**: 289–303.

Raskina O, Barber JC, Nevo E, Belyayev A. 2008. Repetitive DNA and chromosomal rearrangements: speciation-related events in plant genomes. *Cytogenetic and Genome Research* **120**: 351–357.

Schmidt T, Schwarzacher T, Heslop-Harrison JS. 1994. Physical mapping of rRNA genes by fluorescent *in situ* hybridization and structural analysis of 5S rRNA genes and intergenic spacer sequences in sugar beet (*Beta vulgaris*). Theoretical and Applied Genetics **88**: 629–636.

Schmidt A, Doudrick RL, Heslop-Harrison JS, Schmidt T. 2000. The contribution of short repeats of low sequence complexity to large conifer genomes. *Theoretical and Applied Genetics* **101**: 7–14.

Schubert I. 1992. Telomeric polymorphism in *Vicia faba*. *Biologisches Zentralblatt* **111**: 164–168.

Schubert I. 2007. Chromosome evolution. *Current Opinion in Plant Biology* **10**: 109–115.

Schubert I, Lysak MA. 2011. Interpretation of karyotype evolution should consider chromosome structural constraints. *Trends in Genetics* **27**: 207–216.

Schubert I, Wobus U. 1985. *In situ* hybridization confirms jumping nucleolus organizing regions in *Allium*. *Chromosoma* **92**: 143–148.

Schubert I, Rieger R, Fuchs J. 1995. Alteration of basic chromosome number by fusion–fission cycles. *Genome* **38**: 1289–1292.

Slijepcevic P. 1998. Telomeres and mechanisms of Robertsonian fusion. *Chromosoma* **107**: 136–140.

Sousa A, Fuchs J, Renner SS. 2013. Molecular cytogenetics (FISH, GISH) of *Coccinia grandis*: a ca. 3 myr-old species of Cucurbitaceae with the largest Y/autosome divergence in flowering plants. *Cytogenetic and Genome Research* **139**: 107–118.

Souza LGR, Crosa O, Guerra M. 2010. Karyological circumscription of *Ipheion* Rafinesque (Gilliesioideae, Alliaceae). *Plant Systematics and Evolution* **287**: 119–127.

Souza LGR, Crosa O, Winge H, Guerra M. 2009. The karyotype of *Nothoscordum arenarium* Herter (Gilliesioideae, Alliaceae): a populational and cytomolecular analysis. *Genetics and Molecular Biology* **32**: 111–116.

Stamatakis A. 2006. RAxML-VI-HPC: maximum likelihood-based phylogenetic analyses with thousands of taxa and mixed models. *Bioinformatics* **22**: 2688–2690.

Stamatakis A, Hoover P, Rougemont J. 2008. A rapid bootstrap algorithm for the RAxML web-servers. *Systematic Biology* **57**: 758–771.

Tamura K, Peterson D, Peterson N, Stecher G, Nei M, Kumar S. 2011. MEGA5: molecular evolutionary genetics analysis using maximum likelihood, evolutionary distance, and maximum parsimony methods. *Molecular Biology and Evolution* **28**: 2731–2739.

Weiss-Schneeweiss H, Tremetsberger K, Schneeweiss GM, Parker JS, Stuessy TF. 2008. Karyotype diversification and evolution in diploid and polyploid South American *Hypochaeris* (Asteraceae) inferred from rDNA localization and genetic fingerprint data. *Annals of Botany* **101**: 909–918.

White TJ, Bruns T, Lee S, Taylor J. 1990. Amplification and direct sequencing of fungal ribosomal RNA genes for phylogenetics. In: Innis MA, Gelfand DH, Sninsky JJ, White TJ, eds. *PCR protocols: a guide to methods and applications*. New York: Academic Press, 315–322.

Zhin-Ling D, Shao-Tian C, Yun-Heng J, Heng L. 2007. *Typhonium baoshanense* Z. L. Dao & H. Li, a new species of Araceae from western Yunnan, China. *Acta Phytotaxonomica Sinica* **45**: 234–238.

Zhonglang WHL, Fuhua B. 2002. *Typhonium jinpingense*, a new species from Yunnan, China, with the lowest diploid chromosome number in Araceae. *Novon* **12**: 286–289.